Annu. Rev. Environ. Resour. 2003. 28:1–28
doi: 10.1146/annurev.energy.28.050302.105444

First published online as a Review in Advance on July 16, 2003

# CLIMATE CHANGE, CLIMATE MODES, AND CLIMATE IMPACTS

Guiling Wang[1] and David Schimel[2]
[1]*Department of Civil and Environmental Engineering, University of Connecticut, Storrs, Connecticut 06269; email: gwang@engr.uconn.edu*
[2]*Terrestrial Science Section, National Center for Atmospheric Research, Boulder, Colorado 80307; email: schimel@ucar.edu*

**Key Words** North Atlantic Oscillation, El Niño-Southern Oscillation, Pacific Decadal Oscillation, ecosystem response, global warming

■ **Abstract** Variability of the atmospheric and oceanic circulations in the earth system gives rise to an array of naturally occurring dynamical modes. Instead of being spatially independent or spatially uniform, climate variability in different parts of the globe is orchestrated by one or a combination of several climate modes, and global changes take place with a distinctive spatial pattern resembling that of the modes-related climate anomalies. Climate impact on the dynamics of terrestrial and marine biosphere also demonstrates clear signals for the mode effects. In this review, we view modes as an important attribute of climate variability, changes, and impact and emphasize the emerging concept that future climate changes may be manifest as changes in the leading modes of the climate system. The focus of this review is on three of the leading modes: the North Atlantic Oscillation, the El Niño-Southern Oscillation, and the Pacific Decadal Oscillation.

CONTENTS

## INTRODUCTION

Climate can be defined by the long-term statistics that describe the behavior and structure of the Earth's atmosphere, hydrosphere, and cryosphere. Life on the Earth depends on the hospitality of its climate. Any change in the Earth's climate will have an immediate impact on humankind, on biodiversity, and on the health and services delivered by ecosystems around the globe, and it will alter the ability of the earth system to support socioeconomic development. For adaptation to and mitigation of climate changes, it is essential to understand the natural variability of climate, why and how climate changes, and how changes of climate impact the Earth's ecosystems. Recent historical data indicates that the Earth's climate is changing, and such changes tend to take place with a distinctive spatial pattern(s) that may be characterized by one or several modes (repeating patterns of time-space variability) of the climate system. In this review, we discuss climate modes as an important way of understanding climate variability, changes, and impact.

Mode patterns are common and important features of complex dynamical systems. They represent low-dimensional features of high-dimensional systems and provide a better predictive capacity. In meteorology and climatology, "mode" is often used to describe a spatial structure with at least two strongly coupled centers of action. Its polarity and amplitude are represented by the index of the mode, and the temporal variation and changes of the mode index are more predictable than climate anomalies at individual stations. Within the Earth's atmosphere-ocean system, the variability of primary climate variables (e.g., pressure, temperature, and precipitation) gives rise to an array of important, naturally occurring dynamical modes. These include, among many others, the North Atlantic Oscillation (1–3), the Arctic Oscillation and its Southern Hemisphere counterpart, the Antarctic Oscillation (also known as the northern and southern annular modes, respectively) (4–6), the El Niño-Southern Oscillation (1, 2, 7), and the Pacific Decadal Oscillation (8).

Dynamical modes of the climate system result from fundamental physical processes such as "instabilities of the climatological mean flow, large-scale atmosphere-ocean interaction, or interactions between the climatological mean flow and transients" (9). Instead of being spatially independent, large-scale climate variability is often orchestrated by one or several climate modes, which results in synchronized behavior in regions that are geographically far apart. In addition, various data analyses indicated that observed climate changes in the past several decades are statistically related to trends in some of the leading modes, with modal changes explaining a major part of the recent temperature warming. Moreover, numerical modeling studies suggested that future climate changes are likely to occur with a distinctive spatial pattern and are likely to occur as changes in the polarity, frequency, and/or intensity of naturally occurring modes of the climate system.

Modal behavior of the climate system is also manifest in ecological variability and changes over various regions around the globe. In fact, as the first intensively studied climate mode, El Niño was originally noticed in the late nineteenth century by fishermen along the coasts of Ecuador and Peru as a biological phenomenon

in fishery fluctuations, which we now know is caused by El Niño-related oceanic circulation changes resulting in fluctuations of nutrient availability. Climate modes influence the dynamics of both the terrestrial and marine biosphere at levels ranging from individual organisms to communities to ecosystems. In face of the expected anthropogenic climate changes, it becomes critical to understand and predict how the biosphere will respond. Studying the effects of climate modes on the biosphere is crucial to understanding the physical climate system and its coupling to life on planet Earth.

In the following, we will first review the phenomena and climate anomalies associated with various climate modes. The relationship between mode changes and global climate changes will then be analyzed based on both observational data and numerical modeling results. Finally, the ecological and biological impact of climate modes will be reviewed.

## CLIMATE MODES AND CLIMATE VARIABILITY

### Climate Modes: Phenomena

An important method to define the dominant modes of variability for a certain climate anomaly field is the empirical orthogonal function (EOF) analysis (10), also known as the principal component (PC) analysis, of grid data. For example, the first EOF (EOF1) of a meteorological field defines the spatial pattern of the leading mode for this field in the region of analysis, and the associated PC time series provides an index for the temporal variation of the mode. The spatial patterns of leading EOFs have a certain degree of dependence on the shape of the analysis domain. For example, Arctic Oscillation (5, 6, 11) and its Southern Hemisphere counterpart Antarctic Oscillation (4, 12) correspond to the EOF1 of the sea level pressure (SLP) field of the Northern and Southern Hemispheres, respectively, while North Atlantic Oscillation is identified as the EOF1 of the SLP field over the Atlantic sector (13). Similarly, El Niño Southern-Oscillation and Pacific Decadal Oscillation can be derived from the EOF1 and EOF2, respectively, of the SST field over the entire Pacific Basin (14), and Pacific Decadal Oscillation can also be derived from the EOF1 of North Pacific sea surface temperature (8). Many of the mode indices used later in this chapter are derived from EOF/PC analysis, the fundamental technique in defining and analyzing climate modes. Whenever such a mode index is used, the domain of analysis will be specified.

The distribution of SLP in the Atlantic sector of Northern Hemisphere features a subtropical high-pressure center around 35°N and a high-latitude low-pressure center around 55°N, which cause westerly winds across the midlatitude Atlantic throughout the year. Although the exact location of the pressure centers varies from season to season and from year to year, the high-pressure system is generally centered around the Azores, and the low-pressure system is centered around the Iceland. The North Atlantic Oscillation (NAO) represents a north-south oscillation in

atmospheric mass between the Icelandic low and Azores high (1). During the positive phase of NAO, lower-than-normal surface pressure over the Icelandic to Arctic regions and higher-than-normal surface pressure over the subtropical Atlantic together yield a larger than normal meridional pressure gradient, causing stronger than normal midlatitude surface westerlies across the Atlantic onto Europe. The opposite occurs during the negative phase of NAO. This oscillation system gives rise to the leading mode of climate variability in the Northern Hemisphere. A frequently used index for the NAO variation is the PC time series corresponding to the EOF1 of the extended winter (December through March) SLP field over the Atlantic sector in the Northern Hemisphere. An alternative NAO index is defined as the difference in normalized SLP anomalies between individual stations such as that between Lisbon, Portugal, and Stykkisholmur/Reykjavik, Iceland (3). Figure 1*a* plots the normalized anomalies of both the PC time series and the station-based NAO index, which shows negligible difference between these two.

NAO is sometimes considered as the regional manifestation of the Northern Hemisphere annular mode. The annular modes Arctic Oscillation (AO) and Antarctic Oscillation (AAO) refer to a highly zonally symmetric, north-south oscillation in atmospheric mass and momentum between the polar region and temperate latitudes in each hemisphere (5). These modes are most distinctive in the hemispheric SLP fields and are characterized by a primary center of action over the polar caps and anomalies of opposite polarity in midlatitudes. The opposing anomalies in midlatitudes split into two centers of action: For the AO, one is located in the Atlantic sector, and one is over the Pacific; for the AAO, one is in the western Pacific-Indian Ocean sector, and one is near the tip of South America (15). The positive phase features abnormally low pressure over the polar cap and the surrounding regions and higher-than-normal pressure in the midlatitudes with particularly strong anomalies around the centers of actions. The polarity of SLP anomalies reverses during the negative phase. In the Northern Hemisphere, the strongest teleconnectivity between the Arctic basin and midlatitudes occurs over the Atlantic sector, and the teleconnectivity between the Atlantic and Pacific midlatitudes is weak. A similar lack of strong sectoral coherency is documented for the Southern Hemisphere as well. This raises the possibility that the annular modes may have resulted from the large areal extent and the zonal symmetry of their primary centers of action in the Arctic/Antarctic, rather than coordinated behavior between the centers of action in different sectors. As a result, there has been no consensus in the literature regarding whether they represent dynamically significant modes of variability of the hemispheric circulation (6, 9, 13, 15) or are artifacts of EOF analysis. This is particularly the case in the Northern Hemisphere, where the objectively derived NAO and AO indices are nearly indistinguishable and the climate regression with the NAO and AO indices are remarkably similar (except over the northern Pacific where the impact of other climate modes dominates). In this review, we will not treat the annular modes separately and will refer the leading climate mode of the Northern Hemisphere as NAO, with the understanding that NAO and AO may represent two paradigms of the same phenomenon (9).

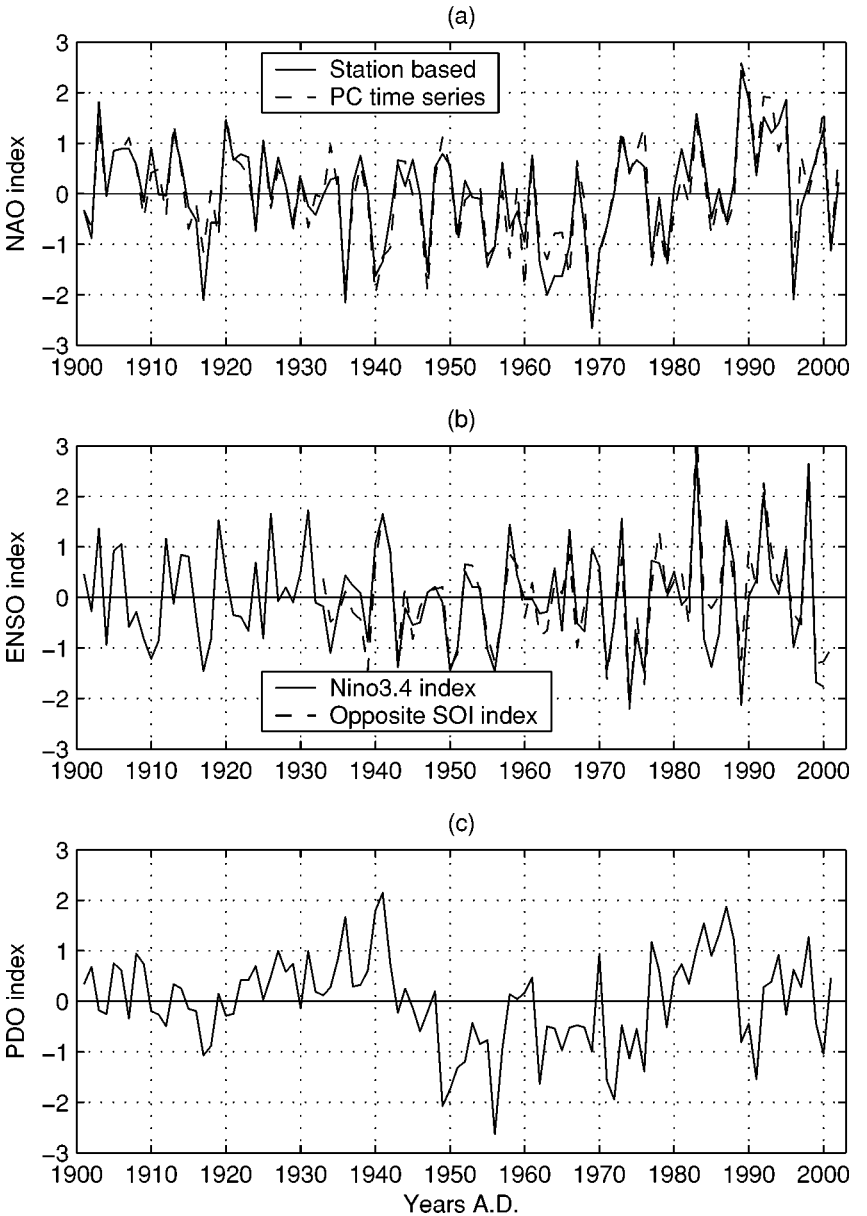


**Figure 1** Normalized time series of (*a*) the NAO index, based on Hurrell (3); (*b*) the ENSO index, based on Trenberth (17) and Trenberth & Hoar (16); (*c*) the PDO index, based on Mantua et al. (8) and Zhang et al. (18).

El Niño-Southern Oscillation (ENSO) is a natural phenomenon arising from the unstable interactions between the tropical Pacific Ocean and the atmosphere. Its oceanic component El Niño (EN) refers to the warm phase of sea surface temperature oscillation in the tropical Pacific Ocean, with the cold phase referred to as La Niña (7). Its atmospheric component the Southern Oscillation (SO) describes a seesaw in atmospheric mass between Eastern and Western Hemispheres in tropical and subtropical latitudes with centers of actions over Australia-Indonesia and the tropical southeastern Pacific (16). Manifestation of ENSO can be found in various meteorological fields across the tropical Pacific, including SLP, trade wind, seas surface temperature, and precipitation, to name a few. Under normal conditions, the trade winds across the tropical Pacific blow toward the west, piling up warm surface water in the West Pacific and causing upwelling of cold water from the ocean depth in the East Pacific off the coast of South America. As a result, sea surface temperature is 6–8°C higher in the west, and convective activities over the warm water bring abundant rainfall to the west. During El Niño, SLP is above normal in the Australia-Indonesia region and below normal in the southeast Pacific; trade wind across the equatorial Pacific relaxes or even reverses; sea surface temperature in central and eastern equatorial Pacific rises significantly; and the major area of precipitation follows the warm water eastward and causes drier-than-normal conditions in the west and wetter-than-normal conditions in the east. The opposite conditions occur during La Niña. Although an index for the ENSO variation can be defined using objective EOF analyses of the Pacific SST field (14), other ENSO indices based on more localized conditions are frequently used. Examples include the Niño3.4 index, defined as the normalized SST anomalies averaged over the Niño3 (5°N-5°S, 150°W-90°W), and Niño4 (5°N-5°S, 160°E-150°W) regions in the equatorial Pacific and the SO index, defined as the difference in the normalized pressure anomalies between Tahiti (T) in the South Pacific and Darwin (D) in northern Australia (i.e., T-D) (16, 17). As such, the warm phase of Niño3.4 (i.e., El Niño) corresponds to the negative phase of the SO (Figure 1*b*). As evidenced in Figure 1*b*, the average timescale of ENSO is approximately four years, with the actual length of cycle ranging from two to seven years.

The Pacific Decadal Oscillation (PDO) refers to a mode of Pacific variability that resembles the ENSO pattern but is dominated by variations at longer timescales (8). The spatial pattern of PDO is qualitatively similar to that of ENSO, with large SST anomalies of one sign in the tropical and northeastern Pacific and anomalies of opposite sign in the central North Pacific (14, 18, 19). The PDO signal is most obvious in the extratropics over North Pacific/North America and weaker in the tropics, as opposed to the ENSO signal that is stronger in the tropics than extratropics. The PC time series corresponding to the EOF1 of Pacific SST poleward of 20N (Figure 1*c*) has been used as a PDO index (8), which shows a preferential timescale of several decades. Due to the difference in their dominant timescale of variations, ENSO is more important in interannual climate variability, and the impact of PDO is more evident in decadal climate variability.

Below, we will focus on the climatic impact of two climate modes, NAO and ENSO, and will also briefly discuss the PDO climate signals. NAO and ESNO are chosen for their extensive areas of significant climate teleconnectivity.

## Impact of NAO on Global Climate Variability

Although the NAO is evident all year long, its impact is particularly strong during boreal winter (20), with NAO-related patterns of temperature and precipitation variability "extending from Florida to Greenland and from northwestern Africa over Europe far into northern Asia" (21). To further demonstrate this, we plot in Figure 2 the correlation coefficient between NAO index and global surface temperature as well as precipitation during Northern Hemisphere winter (December-March). Here, the station-based NAO index as shown in Figure 1*a* (i.e., the difference between the normalized SLP anomaly during winter at Lisbon, Portugal, and Stykkisholmor, Iceland) is used. The global surface temperature dataset (22) has a resolution of 5 degrees in both latitudinal and longitudinal directions and comprises surface air temperature over land and SST over ocean. The correlation analysis was conducted for the time period 1951–2000. For precipitation data, we use the CAMS-OPI data (23), a merged precipitation dataset based on both rain gauge measurements and satellite estimates for the period 1979–2001 with a resolution of 2.5 degrees.

Surface temperatures over much of the Northern Hemisphere are significantly correlated with the NAO index, as is evident in Figure 2*a*. During the positive phase of the NAO, the enhanced high-pressure system over midlatitudes and low-pressure system over Iceland cause both the cyclonic and the anticyclonic winds to become stronger than normal, which leads to enhanced midlatitude westerly winds across the North Atlantic, enhanced southerly winds in the eastern United States and northwestern Europe, and enhanced northerly winds over the Mediterranean, western Greenland, and its surrounding regions (24). The strong westerlies carry mild air from the ocean downwind, causing warmer winter conditions across Europe all the way to northern Asia. At the same time, the enhanced northerlies (southerlies) bring cold (warm) air southward (northward). As a result, colder-than-normal winter conditions occur over Greenland, northeastern Canada, northwest Atlantic, North Africa, and the Middle East, while the majority of the United States and the region poleward from the northwest Europe experience warmer-than-normal winters (Figure 2*a*). A relatively strong cold anomaly develops during the positive phase of the NAO over the Atlantic Ocean between the equator and 30°N, due to the stronger-than-normal northeasterly wind that increases the heat loss from ocean surface to atmosphere. The NAO impact on temperature beyond the Northern Hemisphere is generally weak, with an exception over the midlatitude Southern Hemisphere ocean where summer is warmer than normal during the positive phase of the NAO.

Atmospheric circulation changes associated with the NAO variability lead to pronounced shift of the winter storm track as well as changes of storm frequency

in the Euro-Atlantic sector, which is accompanied by changes in precipitation distribution as demonstrated in Figure 2*b*. Specifically, during the positive phase of the NAO, winter storm activities shift toward the northeast, which causes precipitation to decrease in the south and west and increase in the north and east (25). As a result, drier-than-normal winter conditions are observed over southern Europe, the northern Mediterranean region, part of North Africa, Greenland, and the northeast North America, while more snow falls over the region from Iceland to Scandinavia and northern Europe where winters are stormier during the positive phase of the NAO (3, 26–28). Such NAO-related changes of precipitation are also evident in the swing of river runoff (29) and in the advance and retreat of glaciers (30) and sea ice (31).

## Climatic Impact of ENSO and PDO

Although its primary centers of action are located over the tropical Pacific, ENSO has significant climatic effects over the globe. In fact, most of the interannual variability in the tropics and a substantial portion of the extratropics over both hemispheres are orchestrated by ENSO. Using as the ENSO index the standardized PC time series corresponding to the EOF1 of tropical Pacific SSTs (positive index corresponding to SST warming/El Niño), Figure 3 [modified from Plate 1 and 2 in Diaz et al. (32)] shows the correlation coefficient between the ENSO index and global surface temperature as well as precipitation in different seasons. During the warm phase of ENSO, a general tropical-wide warming is observed all year long, except over part of the Maritime Continent where cooler-than-normal condition occurs during the ASO season (Figure 3*a*,*c*). In the Pacific Ocean, strong tropical warming is flanked by extratropical cooling during all seasons. The southeastern United States experiences cold anomalies in El Niño years, especially during Northern Hemisphere winter. In the extratropics, the strongest correlation between ENSO index and surface temperature occurs in the North Pacific-North America region, where northwestern North America and northeastern Pacific experience significant El Niño-induced warming while cooling occurs over the rest of the North Pacific.

Compared with its impact upon surface temperature, the impact of ENSO on precipitation demonstrates greater spatial variability (Figure 3*b*,*d*). Rainfall increase in the narrow equatorial belt across the Pacific is significantly correlated with El Niño. This is accompanied by rainfall decrease over both the South and North Pacific. Over land, strong drought anomaly in response to El Niño is evident in the Central America, northeastern South America, the Maritime Continent, Australia, and the Indian monsoon region, while wet anomaly occurs over the southern part of both North and South Americas. The ENSO signal over the above-mentioned regions is either seasonally persistent or most pronounced during the local rainy season (32), which leads to a similarity between the relation of ENSO index with seasonal rainfall amount (as shown in Figure 3*b*,*d*) and that with the annually accumulated rainfall amount (33). Substantial seasonal contrast in the response of

precipitation to ENSO is observed in part of East Africa (approximately over the Nile River Basin) and South Africa; each features drier-than-normal conditions in the corresponding rainy season and wetter-than-normal conditions in the corresponding dry season during El Niño years (Figure 3*c*,*d*). The impact of ENSO on precipitation is also reflected by consistent relationships between ENSO and river discharges. For example, during or immediately following El Niño years, stream flow tends to be abnormally low in the Nile River (34, 35), Ganges River (36), Amazon River (37), and River Murray (38, 39), and abnormally high in rivers across the southern United States (40).

The correlation coefficients between the PDO index and global surface temperature and precipitation during the Northern Hemisphere extended winter (December–March) are presented in Figure 4. These correlation analyses use the global surface temperature data of Jones et al. (22) during 1951–2000 and the CAMS-OPI precipitation data (23) during the period 1979–2001; the PDO index used here is the PC time series corresponding to the EOF1 of the Pacific SST poleward of 20°N as shown in Figure 1*c*. The length of data record used in analyzing the correlation of PDO with each climate variable is comparable to that used in the ENSO-climate correlation analysis done by Diaz et al. (32) (and shown in Figure 3). It is clear from Figures 3*a*,*b* and 4*a*,*b* that, compared with the ENSO signal, the PDO signal is stronger in the extratropics and weaker in the tropics. Most noticeable in Figure 4 is the strong correlation between PDO index and temperature in the Pacific-North America region that features cooling in central North Pacific and warming over northwestern North America during the positive phase of PDO.

In summary, from studies reviewed in the two previous sections, it is clear that climate variability in different regions around the globe is not spatially independent. Instead, it tends to be orchestrated by one or the combination of several leading dynamical modes. Except over the North Pacific where the PDO signal is extremely strong, climate variability in the middle- and high-latitudes of Northern Hemisphere is dominated by the NAO. In the tropics and Southern Hemisphere extratropics, ENSO is the dominant forcing of climate variability.

## CLIMATE CHANGES: RELATIONSHIP WITH THE LEADING MODES

Global mean climate in the twentieth century features a significant decadal trend. This is most manifest in temperature warming (22) and to a lesser degree in the intensification of the hydrological cycle (41). Much of this trend is attributable to the rapid changes observed over the past two to three decades. Figure 5 plots the departure of global average temperature from its 1951–1980 mean (42), which shows a dramatic warming trend since the 1970s. Proxy data indicate that the 1990s was likely to be the warmest decade during the past 1000 years (43). The rapid warming in the last three decades of the twentieth century coincides with

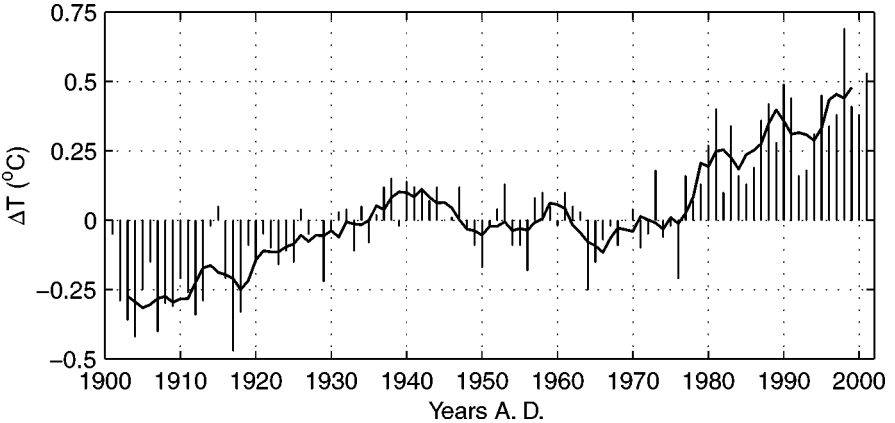


**Figure 5** Global-average surface temperature anomaly with respect to the 1951–1980 climatology, based on the meteorological station analysis of the Goddard Institute for Space Studies by Hansen et al. (42). The heavy solid line plots the 5-year moving average.

a trend or phase shift in several leading modes of climate variability. Since the 1970s, both the NAO and PDO have been developing toward a more positive phase (Figure 1*a*,*c*), and El Niño events have become more frequent (or persistent) and intense (Figure 1*b*). This raises an interesting perspective that climate changes may be expressed as a phase shift or structure change of naturally occurring modes of climate variability and suggests that modes may be a crucial attribute of global climate changes.

## Observed Changes in the Recent Past

Although climate changes are often described by global mean trend, these changes, instead of being uniform in time and space, take place with considerable seasonality and distinctive spatial patterns (44). During the last two decades of the twentieth century, the strongest warming has been observed during the winter and spring seasons in the mid- and high-latitudes of Northern Hemisphere continents, which include the northwestern part of North America, northern Eurasia, and Siberia (20). Little warming or even slight cooling has taken place in part of the northern oceans, including the central North Pacific and northwestern North Atlantic. Most of the Mediterranean region and part of North Africa also witnessed slight cooling impact. This spatial pattern is evident in Figure 6*a*, which shows the departure of surface temperature averaged during 20 recent winters (1981–2000) from the previous 20 winters (1961–1980). In the Southern Hemisphere, little warming has been observed.

The spatial patterns of recent temperature changes are associated with climate anomalies related to changes in the primary modes of atmospheric and/or oceanic

variability, mainly the NAO and to a lesser degree ENSO and PDO. Figure 6*b* and 6*c* present the linear regression of local surface temperature upon the winter NAO and PDO indices, respectively, based on data during the 50-year period 1951–2000. In Figure 6*b*, the largest temperature anomalies associated with the NAO variation occur over the northern Eurasia and Siberia, with a warming of approximately 0.6–1.2°C attributable to a unit increase of the normalized NAO index. The same change of the NAO index accounts for a moderate warming (mostly under 0.6°C) over North America and moderate cooling (mostly under 0.6°C) in eastern Canada, northwest North Atlantic, the Mediterranean, and North Africa. On the other hand, as shown in Figure 6*c*, a strong warming with the magnitude exceeding 1.2 degree centigrade in northwest North America and a moderate cooling in central North Pacific are attributable to a unit increase of the normalized PDO index. Temperature variations accounted for by a unit deviation of the ENSO index (not shown here) and those associated with a unit PDO deviation are broadly similar in their spatial pattern; this indicates that ENSO and PDO explain much of the same climate anomalies. Overall, the spatial distribution of the observed recent climate changes is remarkably similar to that of the NAO-related climate anomalies in Northern Hemisphere except over the Pacific-North America sector where it resembles the spatial distribution of PDO- and ENSO-related climate anomalies.

From the period 1961–1980 to the period 1981–2000, the average of NAO index increases by 1.2 times of its standard deviation and of PDO index by 0.9 (Figure 1). With the correlation coefficient between the NAO and PDO indices not exceeding 0.1, these two time series can be treated as linearly independent. Following the approach of Hurrell (20), subtracting the linear impact of NAO and PDO from the observed temperature changes yields the residual temperature anomalies (Figure 6*d*) that cannot be explained by the variation of these two climate modes. Despite the similarity between climate anomalies associated with PDO and ENSO, PDO is chosen in this analysis because climate over the extratropical Northern Hemisphere is more strongly correlated with the PDO index, as evident in Figures 3 and 4. Replacing the impact of PDO with that of ENSO in this analysis does not cause significant changes in the results. Comparison between Figure 6*a* and 6*d* suggests that most of the observed rapid warming during the past several decades in the extratropical Northern Hemisphere can be accounted for by changes in the naturally occurring modes of climate variability such as the NAO, PDO, and ENSO.

Analysis of global precipitation changes is difficult due to the lack of high-quality data. No precipitation data over the global ocean existed prior to 1980 when satellite-based measurement became available; long-term (multi-decadal) station records of precipitation over land, where they do exist, suffer from various factors such as gauge undercatch and instrumental and technique discontinuity. Therefore, global precipitation changes cannot be estimated with the same level of confidence as temperature changes. Nevertheless, collection of gauge data over the global land does indicate a general, though unsteady, trend of precipitation increase during the twentieth century (26, 45); this is consistent with the temperature warming that promotes a more intense hydrological cycle. It is noteworthy that the increasing

trend of global land precipitation is small relative to its interannual and multidecadal variability. Although the type of global analysis for precipitation changes similar to the one done for temperature changes shown in Figure 6 is not conducted here due to limited spatial and temporal data coverage, localized analyses suggest the link of precipitation changes with observed trends of climate modes, of the NAO and ENSO in particular, as shown below.

In the past two to three decades, most of the precipitation increase has been observed in the Northern Hemisphere mid- and high-latitudes. Conditions over the majority of North America, northern Europe, and Scandinavia have become significantly wetter than normal (44–46), while a general drying trend has been noticed in the Mediterranean region, North Africa, southern Europe, part of northeast Canada, and south Greenland (47, 48). For example, above-normal winter precipitation over Scandinavia is considered responsible for the positive mass balance of the local maritime glaciers (30), snow depth and duration of snow cover over the Alps in the 1990s are at the lower end of their record (49), and severe drought has also been documented for part of Spain and Portugal. Such an increasing trend of precipitation in northern Europe and Scandinavia and decreasing trend to the south as well as over the land mass surrounding northwest Atlantic Ocean are consistent with the northeastward shift of Atlantic storm track resulting from changes of the NAO toward a stronger positive polarity. Precipitation increase in North America, especially over the south and southeast United States, may be related to the development of ENSO and/or PDO toward a more positive phase.

Precipitation data from islands in tropical oceans indicate a coherent decreasing trend over large parts of the tropical oceans but with considerable spatial variability. In particular, most of the eastern Pacific islands exhibit an increasing trend of precipitation, while the western Pacific islands have a decreasing trend (45). This east-west contrast in precipitation changes over the tropical Pacific, which resembles the El Niño-induced anomalies in precipitation distribution, is likely to be related to the increase in the frequency and/or intensity of El Niño events during the recent past (Figure 1*b*).

## Causes for Changes: A Modeling Perspective

It has long been speculated that observed climate changes, the rapid surface warming in particular, during the last two to three decades of the twentieth century may have resulted from the accumulation of anthropogenic greenhouse gases in the atmosphere. On the other hand, as evidenced from the above review, most climate anomalies in the recent past can be accounted for by the observed trend in the natural modes of atmospheric (and oceanic) circulation. This raises the possibility that the recently observed rapid temperature warming may be due to natural climate variability instead of related to the increased greenhouse gas concentration. However, another possibility, which reconciles the above two perspectives, is that increase of greenhouse gas concentration may have caused the observed decadal trend in the naturally occurring modes of climate variability, and that

anthropogenic climate changes may be manifest as changes in the preferred modes of low-frequency climate variability. If this is true, observed modal trends (e.g., the upward trend of the NAO and ENSO indices) are expected to continue into the future as greenhouse gas concentration keeps rising. Currently, due to the short period of record, it is difficult to assess based on observational data whether these trends are anthropogenically induced or are part of the natural decadal variability that coincide with the increase of greenhouse gas concentration. Climate models can be a useful tool to gain some insight regarding possible causes of recent modal changes and their implication for future climate.

Many studies on the response of global climate to past and projected future $CO_2$ concentration increase, which used different coupled atmosphere-ocean general circulation models (AOGCM), found an El Niño-like pattern in $CO_2$-induced climate changes, including changes in surface temperature, precipitation, and SLP (50–54). This pattern is characterized by a larger degree of SST warming in the central and eastern tropical Pacific than in the West, an eastward shift of the precipitation zone in equatorial Pacific resulting in precipitation reduction in western Pacific and increase in central and eastern Pacific, higher pressure over Australasia, and lower pressure over the tropical eastern Pacific. Such climate change patterns reflect changes of the model-simulated ENSO system as $CO_2$ concentration increases and include more frequent and/or more intense El Niño events than La Niña events. These modeling results support the argument that observed changes in ENSO occurrence during the past several decades may include contributions from human impact. However, several other studies on $CO_2$-induced climate changes found no evidence of El Niño-like warming. For example, Meehl et al. (55) documented the lack of SST east-west gradient changes across the equatorial Pacific in a 1% per year transient $CO_2$ experiment using the National Center for Atmospheric Research climate system model (CSM); Washington et al. (56) showed a similar lack of El Niño-like warming in a set of transient $CO_2$ experiments using the Department of Energy (DOE) Parallel Climate Model (PCM). It is interesting to note that the PCM used in Washington et al. (56) and the version of CSM used in Meehl et al. (55) share the same atmospheric component. Discrepancy between different studies may have risen from differences in the parameterization of certain physical processes such as cloud feedback (54) between different climate models.

While the NAO phenomenon and its climatic impact are largely constrained in the extratropics, a recent modeling study by Hoerling et al. (57) found that the observed trend of NAO toward its positive phase in the past several decades may be of tropical origin. Using an atmospheric general circulation model driven with observed SST forcing, this study showed that progressive warming in the tropical Indian and Pacific Oceans modifies the magnitude and spatial pattern of tropical rainfall and thus atmospheric latent heating, which then cause changes in extratropical atmospheric circulation, including the trend of NAO toward a more positive phase in the past several decades. As the observed tropical SST warming is very likely a result of $CO_2$ concentration increase, the Hoerling et al. study provides a piece of evidence, although indirect, that the upward trend of

NAO and the associated warming in mid- to high-latitude Northern Hemisphere constitute an anthropogenic signal. Using coupled AOGCM driven with realistic greenhouse gas forcing, Shindell et al. (58) reproduced the observed trend of the AO (the hemispheric scale counterpart of NAO) when stratospheric dynamics was included in the model. Their results directly demonstrated that the recent trend in AO/NAO and the surface temperature warming associated with it should be attributed to human activities instead of to climate natural variability. It is also indicated in their study that stratospheric dynamics is important to the simulation of anthropogenically induced climate changes. Another study using a different suite of coupled AOGCMs, carried out by Paeth et al. (59), documented that both the NAO mean and its variance are sensitive to greenhouse gas forcing; the former increased while the latter decreased with the increase of $CO_2$ concentration. It was suggested that these two contrasting responses may serve as an indicator for greenhouse gas–induced regional climate changes. However, similar to the simulated ENSO response, not all models agree on how the NAO may respond to $CO_2$ concentration changes. For example, Fyfe et al. (60) argued that the upward trend of the AO/NAO simulated in their coupled AOGCM with greenhouse gas forcing reflects essentially unchanged mode variations superimposed on a forced climate change pattern.

Modal changes related to the greenhouse gas forcing involve more than changes in the polarity, frequency, and/or intensity. They can also be manifest in the spatial pattern of climate anomalies associated with a specific mode. For example, in a transient greenhouse gas experiment using the DOE PCM (B04.29) where $CO_2$ concentration increases by 1% per year from 355 ppmv to 710 ppmv (Figure 7*a*), the NAO develops toward a less negative (or more positive) phase (Figure 7*b*). Figure 8 shows the correlation coefficient between the NAO index and climate anomalies in the Northern Hemisphere winter, based on model simulation for the 30 years right before the onset of $CO_2$ increase in PCM (i.e., concentration fixed at 355 ppmv, labeled as Control) (Figure 8*a–c*) and the 30 years after the stabilization of $CO_2$ concentration at 710 ppmv (labeled as $2 \times CO_2$) (Figure 8*d–f*). For the control simulation, the correlation between the model NAO index and temperature (T) as well as precipitation (P) broadly resembles that based on observations (Figure 2*a*,*b*). The freshwater flux (i.e., P-E, where E stands for evaporation or evapotranspiration), which impacts ecological responses by controlling salinity in the ocean and plant water availability over land, correlates with the NAO in essentially the same manner as precipitation does. Relative to the control, the NAO-climate correlation at $2 \times CO_2$ is generally weaker. In some regions, the spatial pattern of the correlation coefficient at elevated $CO_2$ is considerably different than at the control $CO_2$ level. For example, over the southern United States, wetter-than-normal conditions correspond to the positive phase of the NAO in the control, but drought is expected during the positive phase of the NAO in the $2 \times CO_2$ experiment. The opposite occurs in the northwest United States. Such spatial pattern changes in mode-related climate anomalies are potentially more important than the rather gradual changes in the modal polarity and may pose dramatic impact on regional environment and resources.

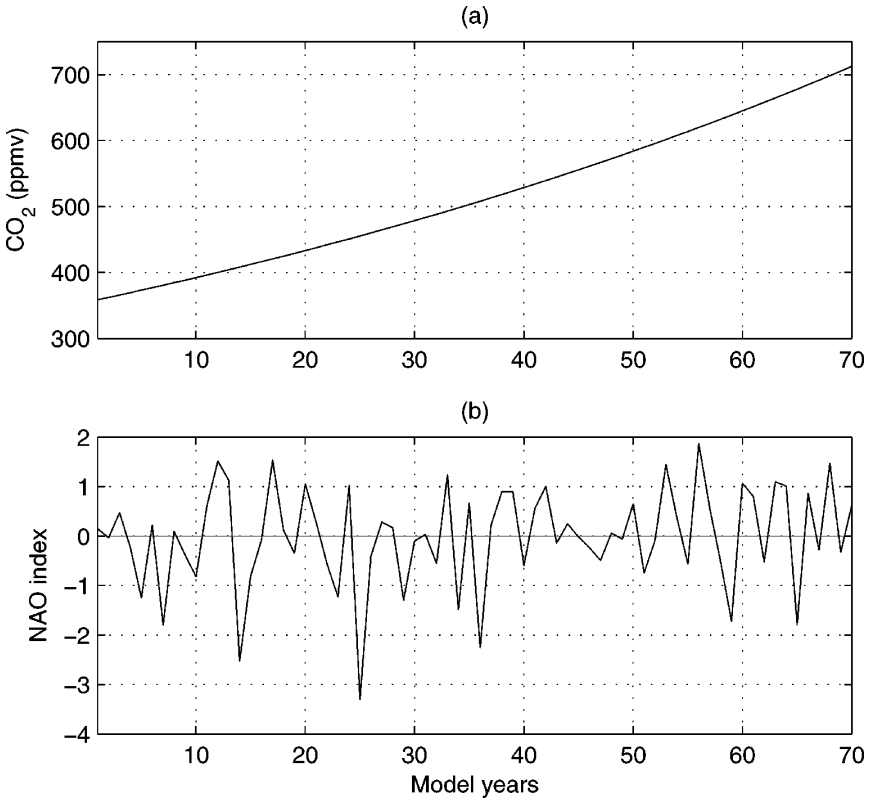


**Figure 7** (*a*) $CO_2$ concentration increase (at 1% per year) and (*b*) the simulated NAO index in the DOE PCM transient $CO_2$ experiment B04.29. Here the NAO index is defined as the difference in normalized anomalies of simulated SLP between Azores and Iceland.

Overall, there exists ample evidence from both observations and numerical modeling studies that anthropogenic climate changes may occur through changes in the preferred modes of atmospheric and/or oceanic circulation. At the same time, it is important to recognize that no conclusive remarks can be made before a longer observational record becomes available, and the model dependence of the simulated modal response to greenhouse gas forcing cannot be overlooked. Further intercomparison study involving multiple global climate models is necessary in order to address such model dependence and to improve our understanding of the modal response to $CO_2$ concentration changes. However, despite the documented discrepancy between different studies, the notion that anthropogenic climate changes may take place as changes in the preferred modes of atmospheric/oceanic circulation represents a potentially significant concept, i.e., greenhouse gases, in addition to their direct radiative effects, may cause significant climate changes through dynamical effects as well.

## CLIMATE MODES AND ECOLOGICAL IMPACTS

Variations in climate modes tend to produce correlated changes in physical variables. For example, ENSO produces spatially structured changes in temperature, precipitation, and cloud cover. Changes in westerly winds associated with the NAO not only change heat transport, they alter patterns of water vapor transport and lead to hydrological cycle changes (24). First-order changes in atmospheric circulation associated with mode changes that produce changes in heat and water transport often result in changes to smaller-scale events in the climate system, and they may change storm frequency, droughtiness, and the frequency of high wind events (see above). Climate modes thus produce correlated changes in multiple physical variables, which include temperature, rainfall, and solar radiation, and also in statistical variables, such as storm frequency and severity as well as precipitation frequency and intensity.

Most literature on climate change impact has focused on the impacts of a single variable (e.g., temperature), or on several variables changing independently in a sensitivity analysis, or on a correlation structure derived from a climate model (61–64). These approaches differ significantly from the syndromes of changes associated with changes to climate modes. In fact, analyses using ecosystem models suggest that biological and hydrological systems are more sensitive to changes in energy balance and water balance (65) arising from changes to heat and water budgets than to temperature or precipitation per se (66). For example, correlated increases in both temperature and rainfall can have a qualitatively different effect than changes in each variable separately. Anti-correlated changes can have complex effects: increases in rainfall (and cloudiness) are often accompanied by decreases in solar radiation for photosynthesis-producing counteracting effects (67, 68). If temperature also decreases (due to reduced radiation), this will affect both photosynthesis and radiation. Effects of changing physical variables on plant and animal phenology and reproduction can also be influenced by these changes, again in complex ways (69). Furthermore, some of the strongest evidence for links between modal variability and ecological responses comes from marine systems in which effects of modes are propagated not only through temperature, but also through ocean circulation changes (70).

Studying the response of the living parts of the earth system to modal variability has two advantages. First, mode shifts provide a geophysical experiment in which climate variables and correlations change systematically, regionally, and with persistence. Second, as discussed above, future climate change may manifest itself partly as changes in the frequency of certain model patterns (for example, a persistently strengthened NAO or more frequent ENSO), and so examining responses to present-day mode shifts is intrinsically useful (71). Below, we review the literature on responses of ecological processes to changes in modal patterns with a focus on reproductive and population responses, seasonality, phenology, productivity, disturbance, and biogeochemistry.

## Population and Reproductive Responses

It has become apparent that climate variability can have a major influence over ecological processes. Modes such as the ENSO, NAO, or PDO can be used as proxies for the actual climate drivers affecting ecosystems and produce clear correlations with biological responses at individual, community, and ecosystem levels. Variation due to climate modes often significantly affects the timing of ecological events. For example, plant phenology is often influenced by modal variation. Williamson & Ickes (72) showed that fruiting of mast-fruiting tropical trees (Dipterocarpaceae) in Southeast Asia was triggered by ENSO events, so that fruiting tended to be synchronized. ENSO events produce significant mortality, which creates a favorable environment for seedling success. In addition, synchronized mass fruiting may increase survivorship by satiating frugivores. They suggest that ENSO-synchronized fruiting may be an evolutionary response to the combination of seedling environment and predator response. Because these trees live far longer than the typical ENSO cycle and are themselves hosts of a wide range of organisms, the ENSO cycle can create periodic phenomena that are triggered by the ENSO cycle but have far longer periods. The linkage between ENSO and mast-fruiting of tropical trees was also reported by other studies (73). The spatial correlation in climate anomalies created by modes has been demonstrated in a wide range of environments. Post & Forchhammer (74) showed populations of musk oxen and caribou on opposite coasts of Greenland were synchronized because the population dynamics were entrained by the same environmental variation. In this case, the driving mode was the NAO that caused coupled population dynamics between groups of organisms separated by a 1000 km of inland icecap. Post & Stenseth (75) showed detailed links between the NAO, plant phenology, and the population dynamics of ungulates in North America and northern Europe. They analyzed 137 time series for plant phenology and showed significant correlation between the NAO and the timing of early blooming. Although there were differences in sensitivity between different functional groups of plants (woody vs. herbaceous and early vs. late bloomers), most species phenology showed correlations with the NAO. In the same study, they analyzed time series of ungulate populations and found strong correlations between NAO and ungulate body size and fecundity. They identified differences between inland and maritime populations. The trigger associated with most NAO effects seemed to be warmer and wetter winters, and surprisingly, they found much stronger effects of wintertime temperatures on animal than plant populations.

Interannual variability due to climate modes can have rather indirect effects. The global decline and local extinctions of amphibians is a well-known phenomenon. Kiesecker et al. (76) showed a potential link to ENSO variability. They found correlations between pathogen outbreaks, amphibian mortality, and the ENSO cycle in the western United States. It was suggested in their study that climate (ENSO drought) conditions in the Pacific Northwest reduced water depths at oviposition sites, which increased UV-B exposure and thus increased susceptibility to the pathogen *Saprolegnia ferax* and hence mortality. The link between *Saprolegnia*

*ferax* susceptibility and UV-B exposure is established, and the correlation between water depths and the Southern Oscillation index is statistically significant in this region. This provides another example of the potential cascading complex of effects between global climate modes, the biophysical environment, and organismal responses. In a rather different study, Morrison & Bolger (77) found effects of both El Niño and La Niña on avian reproductive success. They found relationships between rufous-crowned sparrows and rainfall, with rainfall linked to the ENSO cycle. However, while effects in El Niño years were due to direct effects of rainfall on food, effects in La Niña years were due to altered activity by predators (snakes).

Marine ecosystems show strong links to climate variations. ENSO-induced fluctuation in fishery productivity in the East Pacific is a very well known example, first noticed centuries ago by fishermen along the coasts of Peru and Chile. During El Niño, easterly trade winds across the tropical Pacific slacken or reverse, which slows down the upwelling of cold, nutrient-rich water from the ocean depth in the tropical eastern Pacific. As a result, phytoplankton production drops, which works up the marine food web to eventually reduce fishery productivity (78). Salmon in the North Pacific are influenced by both temperature and circulation changes linked to ENSO and the PDO (shifting fisheries north or south, depending on the phase) and are also affected by drought conditions on land (79). Warmer ocean conditions during El Niño adversely affect chinook and coho salmon. El Niño and PDO also affect the riverine systems used by salmonids for part of their life cycle (8, 80). For example, warmer river water poses a barrier to upstream migration, but low stream flow reduces barriers (such as rapids) that exist at higher flows.

Another important fishery, that of skipjack tuna, is also linked to the ENSO cycle. The skipjack inhabits the Pacific warm pool region, where productivity is low and sea surface temperatures are high. The distribution of skipjack populations is linked to the position of the warm pool and follows it during ENSO years. Interestingly, little is known about the trophic relationships of skipjack, a zooplankton feeder with high energetic demands, and the ecosystem that supports this species. However, hypotheses center on westward transport of plankton communities into a zone of oceanic convergence. The linkage of this trophic system to large-scale transport in the ocean suggests that further research will reveal additional and complex links between pelagic food webs and climate modes. Atlantic fisheries are also linked to climate modes. The NAO appears to be a significant control over recruitment and survival in Atlantic cod. Sirabella et al. (81) showed links between the NAO, temperature, and cod recruitment in the Barents Sea and North Sea. The patterns of correlation suggest a temperature optimum for cod, because in the cold Barents Sea recruitment is directly correlated to temperature (and temperature to the NAO), yet in the warmer North Sea, the correlation is inverse. Chan et al. (82) analyzed a long time series of cod-landing data from Scandinavia in areas where artificial supplementation of larval cod populations had been practiced. They found little evidence for an effect of cod releases on cod populations beyond 6 months of age, but they did find significant dependence across the Norwegian coast of cod populations on the NAO and temperature consistent with the Sirabella et al. (81) findings.

Terrestrial-marine links also exhibit modal variability. Stapp et al. (83) studied island food webs using stable isotopes off Baja California. In these systems, carbon and nutrients from the sea, transported by seabirds and in detritus, support terrestrial communities. In normal years, food webs are based on allochthonous inputs transported from marine sources. In wet El Niño years, rainfall supports flushes of vegetation, and the food webs switch to a terrestrial primary productivity base. In these island ecosystems, climate modes switch the ecosystems from being based on inputs from the sea to being based on in situ terrestrial photosynthesis.

Some of the most complex interactions triggered by modal shifts are in human-environment systems. There now exist a significant number of suggestive case studies linking climate anomalies, ecosystem responses, and human systems (84). In East Africa, a semiarid region, El Niño tends to trigger unusually high rainfall, and this was well documented during the large El Niño of 1997–1998. A complex of cascading effects was documented there (85, 86) in which ENSO-induced changes in vegetation led to significant changes in livestock dynamics. This was of great importance to the semi-traditional pastoral economies of the region with effects that differed, however, by region and elevation. The modulation of the global ENSO phenomenon, first by topographic and ecological differences and then by social systems, resulted in the translation of a common regional process into a host of synchronized but diverse local responses. Increases in precipitation are an anomaly in the drier areas of East Africa and can actually be a stress to human-environment systems well adapted to the prevailing drought conditions (87). Case studies during the 1997–1998 El Niño suggest that negative effects of colder and wetter conditions may actually dominate in parts of East Africa, with increases in both animal and human disease. In Southern Africa, increases in African Horse Sickness (AHS) were found, a disease that affects horses and zebra (88). The virus vector, the biting midge *Culicoides imicola*, breeds in moist soil and can increase dramatically in years of heavy rainfall. Epizootics of AHS occur, typically in ENSO years, but especially in ENSO years when initial drought is followed by heavy rain. The authors suggest that drought causes susceptible animals to congregate near remaining water sources, where, once rains begin, they can both infect vectors and be infected more readily. The El Niño cycle is also linked to human disease. For example, cholera in Bangladesh follows the ENSO cycle closely, probably because of links between disease processes and temperature, but it is also possibly because of changes to the large-scale hydrological cycle (89).

## Biogeochemistry, Disturbance, and the Global Carbon Cycle

The first mention of a link between climate modes (El Niño) and biogeochemistry was probably in Bacastow et al. (90) in which they noted a significant relationship between the Mauna Loa $CO_2$ record and the El Niño cycle, suggesting a link between the ocean carbon cycle and atmospheric $CO_2$. This link is one of the most

useful and important pieces of evidence for strong effects of climate on the carbon cycle (71), together of course with the ice core record.

Although the link between ENSO and carbon was first thought to be an oceanic phenomenon (90) due to the marine origins of the El Niño, work in the 1990s showed that the variations were too large to be explained exclusively by marine circulation or temperature changes (91, 92), a conclusion since supported by isotopic analyses (93). Expansion of the tropical warm pool reduces upwelling of cold, $CO_2$-rich water in the tropics during El Niño and should cause an apparent increase in global ocean carbon uptake. Feely et al. (91) supported this argument but showed the observed changes in marine $CO_2$ to be too small to explain the atmospheric variations. Oceanic changes during El Niño may not explain the global carbon cycle correlation, but time-series data from marine process studies suggest profound effects of ENSO on marine biogeochemistry (94), which was also suggested implicitly in fisheries studies, above.

In the 1990s, terrestrial explanations for El Niño-$CO_2$ correlations began to emerge. The Amazon basin experiences droughts during El Niño years. Using a model, Tian et al. (95) suggested that reductions in soil moisture caused increases in respiratory carbon release relative to photosynthetic uptake. Despite model-based analyses, satellite-based studies of terrestrial biosphere primary productivity do not show a clear global signature although regional changes were observed, which suggests that productivity and respiration may not be the only terrestrial process contributing to El Niño-related $CO_2$ variations. Nepstad et al. (96) showed that biomass burning associated with forest clearing was linked to El Niño droughts, due to the flammability of slash. They argued that Amazon basin emissions could double in strong El Niño years.

Vukicevic et al. (97) fit a simple model of the responses of photosynthesis, respiration, and nitrogen cycling to interannual temperature variability. They showed that a significant amount of interannual biogeochemical variability could be explained by ecosystem responses to temperature but that large residuals were associated with El Niño periods. The residuals were negative (uptake) early in the El Niño period and large and positive (emissions) later. This pattern is consistent with ocean uptake early in the El Niño and emissions following as ENSO droughts take hold. New evidence suggests that El Niño droughts may play a major role in the carbon cycle and interact with wildfire. Langenfelds et al. (93) used atmospheric measurements of $CO_2$, $^{13}CO_2$, and several chemical tracers of fire. They found a high degree of correlation between changes to the growth rates of pyrogenic compounds ($H_2$, $CH_4$, and CO) and that of $CO_2$ during time periods in which $^{13}CO_2$ suggested a primarily terrestrial origin for the $CO_2$. Langenfelds et al. (93) concluded that a significant fraction of the interannual variability in carbon cycling during the 1990s was due to wildfire. In parallel studies, several groups began to focus on the extremely large wildfires in Indonesia during the 1997–1998 El Niño. Page et al. (98) estimated that emissions from these fires were between 0.8 and 2.6 Gt of carbon, an amount equal to 13%–40% of global fossil emissions, and similar to total global biospheric storage in a typical year (99). The emissions were

large because of the size and intensity of the fires, and also because they burned through peatlands, where vast amounts of carbon were stored in the soil. While these wildfires were triggered by the El Niño drought, the fires were most severe in regions that were recently logged, where large amounts of flammable material were available and where roads and drainage channels had lowered the water table and allowed the peat soils to burn as well as vegetation. The Indonesian emissions were very large and produced a clearly detectable signal in atmospheric $CO_2$, but additional analysis suggests that other tropical regions were also sources in that El Niño year (100).

## Summary

Recent research has revealed roles for the climate modes in controlling ecosystems at scales ranging from growth, reproduction, and survival of individual organisms through the global carbon cycle. Although the diversity of organisms and ecological processes with documented links to climate modal variation is enormous, a few themes emerge. First, many regional variations in climate are associated with climate mode shifts. These large regional climate shifts are important ecologically for two reasons. First, they tend to produce regional synchrony in biological and/or biogeochemical processes over large regions. Regional synchrony can have population or even evolutionary links (72) due to interactions with density-dependent population processes (75). Regional synchrony can also produce large biogeochemical fluxes as is evident in the ENSO cycle-global carbon cycle correlation. The second, and coupled, theme is the link between climate mode shifts, climate extremes, and ecological responses. Many climate extremes of drought and heavy precipitation are linked to phases of the climate modes. Human and livestock health are linked to El Niño flooding in East Africa (87), barriers to salmon migration are linked to El Niño precipitation variation in the U.S. Pacific Northwest (80), and wildfire impacts on the carbon cycle are linked to El Niño droughts (98). In anticipating the future, climate change impacts are likely to be significantly mediated via changes to the intensity, spatial pattern, or frequency of climate modes. Entirely new impacts could occur if climate change produces new modes or if the spatial domain affected by an existing mode shifts. Research on the impacts of climate modes, typically described as producing variation on seasonal to decadal timescales, is extremely complementary to research on climate change typically thought of as occurring on decadal to centennial timescales.

# FINAL REMARKS

Variations in the Earth's atmospheric and oceanic circulations generate an array of important dynamical modes, which provide an efficient way to study large-scale climate variability, climate impact, and even anthropogenically induced climate

changes. Our review was limited to several of the leading modes, which included the NAO, ENSO, and PDO. These modes were chosen either because of the extensive spatial coverage of their impact or because of their strong impact on a specific region. In addition, ENSO and NAO are also among the most intensively studied modes of the climate system and are therefore better understood than others.

Long-term observational data produced evidence for strong and statistically significant correlations between dynamical modes and regional-global climate variability. The relationships between modes and certain ecological processes in both terrestrial and marine environments are also well established. For both climate variability and ecological impact, the NAO effects dominate over the majority of the Atlantic sector that includes eastern North America, North Atlantic, and Eurasia; the ENSO signal is prominent over the tropics and the majority of Southern Hemisphere extratropics; the PDO plays a significant role in North Pacific and a major part of North America. Therefore, examining the temporal variation of modes may lead to important predictive information for many aspects of regional and global environment and resources, such as winter severity, storminess, water resources, agriculture and fishery productivity, and timing and length of growing season. In particular, the persistence of some climate modes and their link to slowly varying ocean conditions create an opportunity for limited prediction of seasonal climate (101). For example, information from seasonal predictions based on the El Niño cycle is now made available regularly by the International Research Institute for Climate Prediction (http://iri.columbia.edu/) and has significant value for preparing for climate impacts (102, 103). In addition, several studies have demonstrated the potential use of ENSO index as a predictor for the discharge of some major rivers (34–40).

The linkage between modes and climate changes is less definitive. The secular trend found in the global mean surface temperature during the past century is mainly due to the rapid warming since the 1970s, and the majority of these temperature changes can be explained by the trend of NAO and PDO toward a more positive phase and by the more frequent/persistent occurrence of El Niño during the past two to three decades. This suggests that $CO_2$-induced climate changes may manifest through changes in the naturally occurring modes of the climate system. However, before a longer record becomes available, one cannot exclude the possibility that recent modes anomalies might be just part of their long-term variability. Although there has been no consensus among numerical modeling studies, many climate models indicated that increasing greenhouse gas concentration changes the naturally occurring modes of the climate system and supported the linkage between modes and anthropogenic climate changes.

It has long been established that $CO_2$ impacts the global climate through its direct radiative effects. More recent studies indicated that indirect effects through plant physiology and vegetation structure changes are also important (104–106). The perspective that $CO_2$-induced climate changes may take place through changes in the primary dynamical modes implies the potential existence of a third type of effects, i.e., through changes in the atmospheric and oceanic circulation

patterns. This potential linkage between modes and climate changes will also make modes a useful tool for evaluating the regional and global impact of future climate changes.

Although this review focused on recent historical data, information about climate modes is preserved in the paleo-record as well and demonstrates that at least some modern modes are ancient (107). Paleo-record and archeological data also show that modal variability has long had environmental and human consequences (108). Modes are an important factor to consider for climate variability and changes, and their impacts are not limited to modern times.

**The *Annual Review of Environment and Resources* is online at http://environ.annualreviews.org**

## LITERATURE CITED


1. Walker GT, Bliss EW. 1932. World weather V. *Mem. R. Meteorol. Soc.* 4:53–83
2. Wallace JM, Gutzler DS. 1981. Teleconnections in the geopotential height field during the Northern Hemisphere winter. *Mon. Weather Rev.* 109:784–812
3. Hurrell JW. 1995. Decadal trends in the North Atlantic Oscillation: regional temperatures and precipitation. *Science* 269: 676–79
4. Limpasuvan V, Hartmann DL. 1999. Eddies and the annual modes of climate variability. *Geophys. Res. Lett.* 26:3133–36
5. Thompson DWJ, Wallace JM. 1998. The Arctic Oscillation signature in the wintertime geopotential height and temperature fields. *Geophys. Res. Lett.* 25:1297–1300
6. Thompson DWJ, Wallace JM. 2001. Regional climate impacts of the Northern Hemisphere annual mode. *Science* 293:85–89
7. Philander SGH. 1985. El Niño and La Niña. *J. Atmos. Sci.* 42:2652–62
8. Mantua NJ, Hare SR, Zhang Y, Wallace JM, Francis RC. 1997. A Pacific interdecadal climate oscillation with impacts on salmon production. *Bull. Am. Meteorol. Soc.* 78:1069–79
9. Wallace JM. 2000. North Atlantic Oscillation/annular mode: Two paradigms–one phenomenon. *Q. J. R. Meteorol. Soc.* 126:791–805
10. Jolliffe IT. 2002. *Principal Component Analysis*. New York: Springer. 502 pp.
11. Thompson DWJ, Wallace JM, Hegerl GC. 2000. Annual modes in the extratropical circulation. Part II: trends. *J. Clim.* 13: 1018–36
12. Rogers JC, van Loon H. 1982. Spatial variability of sea level pressure and 500-mb height anomalies over the Southern Hemisphere. *Mon. Weather Rev.* 110:1375–92
13. Ambaum MHP, Hoskins BJ, Stephenson DB. 2001. Arctic Oscillation or North Atlantic Oscillation? *J. Clim.* 14:3495–3507
14. Barlow M, Nigam S, Berbery EH. 2001. ENSO, Pacific decadal variability, and U.S. summertime precipitation, drought, and stream flow. *J. Clim.* 14:2105–28
15. Deser C. 2000. On the teleconnectivity of the "Arctic Oscillation." *Geophys. Res. Lett.* 27:779–82
16. Trenberth KE, Hoar TJ. 1996. The 1990–1995 El Niño-Southern Oscillation event: longest on record. *Geophys. Res. Lett.* 23: 57–60
17. Trenberth KE. 1984. Signal versus noise in the Southern Oscillation. *Mon. Weather Rev.* 112:326–332
18. Zhang Y, Wallace JM, Battisti DS.

1997. ENSO-like interdecadal variability: 1900–93. *J. Clim.* 10:1004–20
19. Mantua NJ, Hare SR. 2002. The Pacific Decadal Oscillation. *J. Oceanogr.* 58:35–44
20. Hurrell JW. 1996. Influence of variations ion extratropical wintertime teleconnections on Northern Hemisphere temperature. *Geophys. Res. Lett.* 23:665–68
21. Visbeck MH, Hurrell JW, Polvani L, Cullen HM. 2001. The North Atlantic Oscillation: past, present, and future. *Proc. Natl. Acad. Sci. USA* 98:12876–77
22. Jones PD, Osborn TJ, Briffa KR. 2001. The evolution of climate over the last millennium. *Science* 292:662–67
23. Janowiak JE, Xie PP. 1999. CAMS-OPI: a global satellite-rain gauge merged product for real-time precipitation monitoring applications. *J. Clim.* 12:3335–42
24. Hurrell JW, Kushnir Y, Ottersen G, Visbeck M, eds. 2003. *The North Atlantic Oscillation: Climate Significance and Environmental Impact*. Geophys. Monogr. Ser. 134. Washington, DC: Am. Geophys. Union. 279 pp.
25. Hurrell JW, van Loon H. 1997. Decadal variations in climate associated with the North Atlantic Oscillation. *Clim. Change* 36:301–26
26. Dai AG, Fung IY, Genio ADD. 1997. Surface observed global land precipitation variations during 1900–88. *J. Clim.* 10:2943–62
27. Hartley S, Keables MJ. 1998. Synoptic associations of winter climate and snowfall variability in New England, USA, 1950–1992. *Int. J. Climatol.* 18:281–98
28. Dickson RR, Osborn TJ, Hurrell JW, Meincke J, Blindheim J, et al. 2000. The Arctic Ocean response to the North Atlantic Oscillation. *J. Clim.* 13:2671–96
29. Perreault L, Hache M, Slivitzky M, Bobee B. 1999. Detection of changes in precipitation and runoff over eastern Canada and US using a Bayesian approach. *Stoch. Environ. Res. Risk Assess.* 13:201–16
30. Siggurdson O, Jonsson T. 1995. Relation of glacier variations to climate changes in Iceland. *Ann. Glaciol.* 21:263–70
31. Deser C, Blackmon ML. 1993. Surface climate variations over the North Atlantic Ocean during winter: 1900–1989. *J. Clim.* 6:1743–53
32. Diaz HF, Hoerling MP, Eischeid JK. 2001. ENSO variability, teleconnections and climate change. *Int. J. Climatol.* 21:1845–62
33. Dai AG, Wigley TML. 2000. Global pattern of ENSO-induced precipitation. *Geophys. Res. Lett.* 27:1283–86
34. Eltahir EAB. 1996. El Niño and the natural variability in the flow of the Nile River. *Water Resourc. Res.* 32:132–37
35. Wang GL, Eltahir EAB. 1999. Use of ENSO information in the medium- to long-range forecasting of the Nile flood. *J. Clim.* 12:1726–37
36. Whitaker DW, Wasimi SA, Islam S. 2001. The El Niño-Southern Oscillation and long-range forecasting of flows in the Ganges. *Int. J. Climatol.* 21:77–87
37. Richey JE, Nobre C, Deser C. 1989. Amazon River discharge and climate variability: 1903–1985. *Science* 246:101–3
38. Simpson HJ, Cane MA, Herczeg AL, Zebiak SE, Simpson JH. 1993. Annual river discharge in southeastern Australia related to El Niño-Southern Oscillation forecasts of sea surface temperature. *Water Resourc. Res.* 29:3671–80
39. Simpson HJ, Cane MA, Lin SK, Zebiak SE. 1993b. Forecasting annual discharge of River Murray, Australia, from a geophysical model of ENSO. *J. Clim.* 6:386–90
40. Piechota TC, Dracup JA. 1996. Drought and regional hydrologic variation in the United States: associations with the El Niño Southern Oscillation. *Water Resourc. Res.* 32:1359–73
41. Hulme M, Osborn TJ, Johns TC. 1998. Precipitation sensitivity to global warming: comparison of observations with HadCM2 simulations. *Geophys. Res. Lett.* 25:3379–82

42. Hansen J, Ruedy R, Glascoe J, Sato M. 1999. GISS analysis of surface temperature change. *J. Geophys. Res.* 104:30997–1022
43. Mann ME. 2001. Climate during the past millennium. *Weather* 56:91–101
44. Intergov. Panel Clim. Change. 2001. *Climate Change 2001: The Scientific Basis—Contribution of Working Group I to the Third Assessment Report of the Intergovernmental Panel on Climate Change*, ed. JT Houghton, Y Ding, DJ Griggs, M Noguer, PJ van der Linden, et al. New York: Cambridge Univ. Press. 881 pp.
45. New M, Todd M, Hulme M, Jones P. 2001. Precipitation measurements and trends in the twentieth century. *Int. J. Climatol.* 21: 1899–922
46. Hanssen-Bauer I, Forland E. 2000. Temperature and precipitation variations in Norway 1900–1994 and their links to atmospheric circulation. *Int. J. Climatol.* 20:1693–708
47. Piervitali E, Colacino M, Conte M. 1998. Rainfall over the central-western Mediterranean basin in the period 1951–1995. Part I: precipitation trends. *Nuovo Cimento Della Soc. Italiana Di Fis. C—Geophys. Space Phys.* 21:331–44
48. Romero R, Guijarro JA, Ramis C, Alonso S. 1998. A 30-year (1964–1993) daily rainfall data base for the Spanish Mediterranean regions: first exploratory study. *Int. J. Climatol.* 18:541–60
49. Beniston M. 1997. Variation of snow depth and duration in the Swiss Alps over the last 50 years: links to changes in large-scale climatic forcings. *Clim. Change* 36:281–300
50. Knutson TR, Manabe S. 1995. Time-mean response over the tropical Pacific to increased $CO_2$ in a coupled ocean-atmosphere model. *J. Clim.* 8:2181–99
51. Meehl GA, Washington WM. 1996. El Niño-like climate change in a model with increased atmospheric $CO_2$ concentrations. *Nature* 382:56–60
52. Meehl GA, Washington WM, Arblaster JM, Bettge TW, Strand WG Jr. 2000. Anthropogenic forcing and decadal climate variability in sensitivity experiments of twentieth- and twenty-first-century climate. *J. Clim.* 13:3728–44
53. Boer GJ, Flato G, Ramsden D. 2000. A transient climate change simulation with greenhouse gas and aerosol forcing: projected climate to the twenty-first century. *Clim. Dyn.* 16:427–50
54. Timmermann A, Oberhuber J, Bacher A, Each M, Latif M, Roeckner E. 1999. Increased El Niño frequency in a climate model forced by future greenhouse warming. *Nature* 398:694–97
55. Meehl GA, Collins WD, Boville BA, Kiehl JT, Wigley TML, Arblaster JM. 2000. Response of the NCAR climate system model to increased $CO_2$ and the role of physical processes. *J. Clim.* 13:1879–98
56. Washington WM, Weatherly JW, Meehl GA, Semtner AJ Jr, Bettge TW, et al. 2000. Parallel Climate Model (PCM) control and transient simulations. *Clim. Dyn.* 16:755–74
57. Hoerling MP, Hurrell JW, Xu TY. 2001. Tropical origins for recent North Atlantic climate change. *Science* 292:90–92
58. Shindell DT, Miller RL, Schmidt GA, Pandolfo L. 1999. Simulation of recent northern winter climate trends by greenhouse-gas forcing. *Nature* 399:452–55
59. Paeth H, Hense A, Glowienka-Hense R, Voss R, Cubasch U. 1999. The North Atlantic Oscillation as an indicator for greenhouse-gas induced regional climate change. *Clim. Dyn.* 15:953–60
60. Fyfe JC, Boer GJ, Flato GM. 1999. The Arctic and Antarctic oscillations and their projected changes under global warming. *Geophys. Res. Lett.* 26:1601–4
61. Schimel DS, Parton WJ, Kittel TGF, Ojima DA, Cole CV. 1990. Grassland biogeochemistry—links to atmospheric processes. *Clim. Change* 17:13–25
62. Schimel DS, Braswell BH, McKeown R,

Ojima DS, Parton WJ, Pullian W. 1996. Climate and nitrogen controls on the geography and timescales of terrestrial biogeochemical cycling. *Glob. Biogeochem. Cycles* 10:677–92

63. Schimel D, Melillo J, Tian H, McGuire AD, Kicklighter D, et al. 2000. Contribution of increasing $CO_2$ and climate to carbon storage by ecosystems in the United States. *Science* 287:2004–6
64. Melillo JM, Borchers J, Chaney J, Fisher H, Fox S, et al. 1995. Vegetation ecosystem modeling and analysis project—comparing biogeography and biogeochemistry models in a continental-scale study of terrestrial ecosystem responses to climate-change and $CO_2$ doubling. *Glob. Biogeochem. Cycles* 9:407–37
65. Schimel DS, Emanuel W, Rizzo B, Smith T, Woodward FI, et al. 1997. Continental scale variability in ecosystem processes: models, data, and the role of disturbance. *Ecol. Monogr.* 67:251–71
66. Bachelet D, Neilson RP, Lenihan JM, Drapek RJ. 2001. Climate change effects on vegetation distribution and carbon budget in the United States. *Ecosystems* 4:164–85
67. Tian H, Melillo JM, Kicklighter DW, McGuire AD, Helfrich J. 1999. The sensitivity of terrestrial carbon storage to historical climate variability and atmospheric $CO_2$ in the United States. *Tellus B* 51:414–52
68. Tian H, Melillo JM, Kicklighter DW, McGuire AD, Helfrich J, et al. 2000. Climatic and biotic controls on annual carbon storage in Amazonian ecosystems. *Glob. Ecol. Biogeogr.* 9:315–35
69. Ottersen G, Planque B, Belgrano A, Post E, Reid PC, Stenseth NC. 2001. Ecological effects of the North Atlantic Oscillation. *Oecologia* 128:1–14
70. Sugimoto T, Kimura S, Tadokorol K. 2001. Impact of El Niño events and climate regime shifts on living resources in the western North Pacific. *Prog. Oceanogr.* 49:113–27
71. Cox PM, Betts RA, Jones CD, Spall SA, Totterdell IJ. 2000. Acceleration of global warming due to carbon-cycle feedbacks in a coupled climate model. *Nature* 408:184–87
72. Williamson GB, Ickes K. 2002. Mast fruiting and ENSO cycles—does the cue betray a cause? *Oikos* 97:459–61
73. Curran LM, Caniago I, Paoli GD, Astianti D, Kusneti M, et al. 1999. Impact of El Niño and logging on canopy tree recruitment in Borneo. *Science* 286:2184–88
74. Post E, Forchhammer MC. 2002. Synchronization of animal population dynamics by large-scale climate. *Nature* 420:168–71
75. Post E, Stenseth NC. 1999. Climate variability, plant phenology, and northern ungulates. *Ecology* 80:1322–39
76. Kiesecker JM, Blaustein AR, Belden LK. 2001. Complex causes of amphibian population declines. *Nature* 410:681–84
77. Morrison SA, Bolger DT. 2002. Variation in a sparrow's reproductive success with rainfall: food and predator-mediated success. *Oecologia* 133:315–24
78. Caviedes CN, Fik TJ. 1992. The Peru-Chile eastern Pacific fisheries and climatic oscillations. In *Climate Variability, Climate Change and Fisheries*, ed. MH Glantz, pp. 355–76. Cambridge, UK: Cambridge Univ. Press
79. Francis RC, Hare SR, Hollowed AB, Wooster WS. 1998. Effects of interdecadal climate variability on the oceanic ecosystem of the NE Pacific. *Fish. Oceanogr.* 7:1–21
80. Miller KA, Munro G, McKelvey R, Tyedmers P. 2001. Climate, uncertainty and the Pacific salmon treaty: Insights on the harvest management game. In *Microbehavior and Microresults: Proceedings of the Tenth Biennial Conference of the International Institute of Fisheries Economics and Trade*, ed. RS Johnston, AL Shriver. Corvallis: IIFET
81. Sirabella P, Giuliani A, Colosimo A, Dippner JW. 2001. Breaking down the

climate effects on cod recruitment by principal component analysis and canonical correlation. *Mar. Ecol. Prog. Ser.* 216:213–22
82. Chan K-S, Stenseth NC, Kittilsen MO, Gjoseter J, Lekve K, et al. 2003. Assessing the effectiveness of releasing cod larvae for stock improvement with monitoring data. *Ecol. Appl.* 13:3–22
83. Stapp P, Polls GA, Pinero FS. 1999. Stable isotopes reveal strong marine and El Niño effects on island food webs. *Nature* 401:467–69
84. Glantz MH. 2000. *Currents of Change: Impact of El Niño and La Niña on Climate and Society.* Cambridge, UK: Cambridge Univ. Press. 272 pp. 2nd ed.
85. Boone RB, Galvin KA, Smith NM, Lynn SJ. 2000. Generalizing El Niño effects upon Maasai livestock using hierarchical clusters of vegetation patterns. *Photogramm. Eng. Remote Sens.* 66:737–44
86. Galvin KA, Boone RB, Smith NM, Lynn SJ. 2001. Impacts of climate variability on East African pastoralists: linking social science and remote sensing. *Clim. Res.* 19: 161–72
87. Little PD, Mahmoud H, Coppock DL. 2001. When deserts flood: risk management and climatic processes among East African pastoralists. *Clim. Res.* 19:149–59
88. Baylis M, Mellor PS, Meiswinkel R. 1999. Horse sickness and ENSO in South Africa. *Nature* 397:574
89. Pascual M, Bouma MJ, Dobson AP. 2002. Cholera and climate: revisiting the quantitative evidence. *Microbes Infect.* 4:237–45
90. Bacastow RB, Adams JA, Keeling CD, Moss DJ, Whorf TP, Wong CS. 1980. Atmospheric carbon dioxide, the Southern Oscillation, and the weak 1975 El Niño. *Science* 210:66–68
91. Feely RA, Wanninkhof R, Takahashi T, Tans P. 1999. Influence of El Niño on the equatorial Pacific contribution to atmospheric $CO_2$ accumulation. *Nature* 398: 597–601
92. Lee K, Wanninkhof R, Takahashi T, Doney SC, Feely RA. 1998. Low interannual variability in recent oceanic uptake of atmospheric carbon dioxide. *Nature* 396:155–59
93. Langenfelds RL, Francey RJ, Pak BC, Steele LP, Lloyd J, et al. 2002. Interannual growth rate variations of atmospheric $CO_2$ and its $^{13}C$, $H_2$, $CH_4$, and CO between 1992 and 1999 linked to biomass burning. *Glob. Biogeochem. Cycles* 16: Artic. 1048;10.1029/2001GB001466
94. Karl D, Letelier R, Tupas L, Dore J, Christian J, Hebel D. 1997. The role of nitrogen fixation in biogeochemical cycling in the subtropical North Pacific Ocean. *Nature* 388:533–38
95. Tian HQ, Melillo JM, Kicklighter DW, McGuire AD, Helfrich JVK, et al. 1998. Effects of interannual climate variability on carbon storage in Amazonian ecosystems. *Nature* 396:664–67
96. Nepstad DC, Verissimo A, Alencar A, Nobre C, Lima E, et al. 1999. Large-scale impoverishment of Amazonian forests by logging and fire. *Nature* 398:505–8
97. Vukicevic T, Braswell BH, Schimel D. 2001. A diagnostic study of temperature controls on global terrestrial carbon exchange. *Tellus B* 53:150–70
98. Page SE, Siegert F, Rieley JO, Boehm HDV, Jaya A, Limin S. 2002. The amount of carbon released from peat and forest fires in Indonesia during 1997. *Nature* 420:61–65
99. Schimel DS, House JI, Hibbard KA, Bousquet P, Ciais P, et al. 2001. Recent patterns and mechanisms of carbon exchange by terrestrial ecosystems. *Nature* 414:169–72
100. Schimel DS, Baker D. 2002. Carbon cycle: the wildfire factor. *Nature* 420:29–30
101. Goddard L, Mason SJ. 2001. Sensitivity of seasonal climate forecasts to persisted SST anomalies. *IRI Tech. Rep. 01–04*. Int.

Res. Inst. Clim. Predict., Columbia Univ., Palisades, NY
102. Glantz MH. 2001. Once Burned, Twice shy: lessons learned from the 1997–98 El Niño. Tokyo, Jpn: United Nations Univ. Press, 294 pp.
103. Phillips JG, Deane D, Unganai L, Chimele AB. 2002. Changes in small-holder grain production in Zimbabwe using seasonal climate forecasts. *Agric. Syst.* 74:351–69
104. Betts RA, Cox PM, Lee SE, Woodward FI. 1997. Contrasting physiological and structural vegetation feedbacks in climate change simulations. *Nature* 387:796–99
105. Levis S, Foley JA, Pollard D. 2000. Large-scale vegetation feedbacks on a doubled $CO_2$ climate. *J. Clim.* 13:1212–325
106. Wang GL, Eltahir EAB. 2002. Response of the biosphere-atmosphere system in West Africa to $CO_2$ concentration changes. *Glob. Change Biol.* 8:1169–82
107. Eltahir EAB, Wang GL. 1999. Nilometers, El Niño, and climate variability. *Geophys. Res. Lett.* 26:489–92
108. Sandweiss DH, Maasch KA, Burger RL, Richardson JB, Rollins HB, Clement A. 2001. Variation in Holocene El Niño frequencies: climate records and cultural consequences in ancient Peru. *Geology* 29:603–6

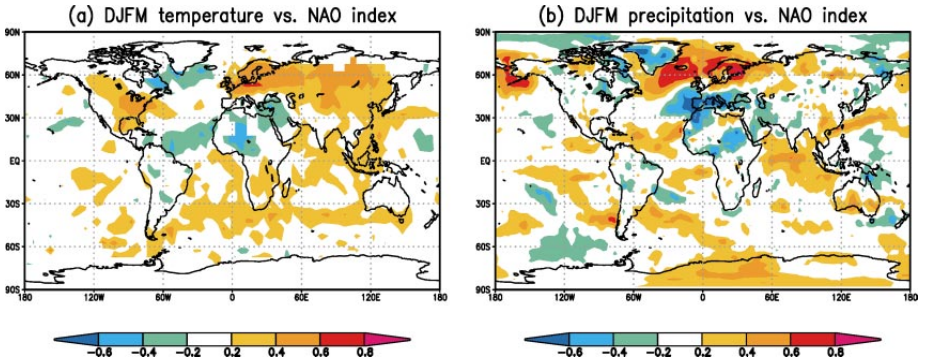


**Figure 2** (*a*) Correlation coefficient between the NAO index and global surface temperature in extended boreal winter December–March (DJFM), based on data during 1951–2000; (*b*) Correlation coefficient between the NAO index and global precipitation in DJFM, based on data during 1979–2001. The 5% significance level corresponds to a correlation coefficient of approximately 0.28 in (*a*) and 0.42 in (*b*).

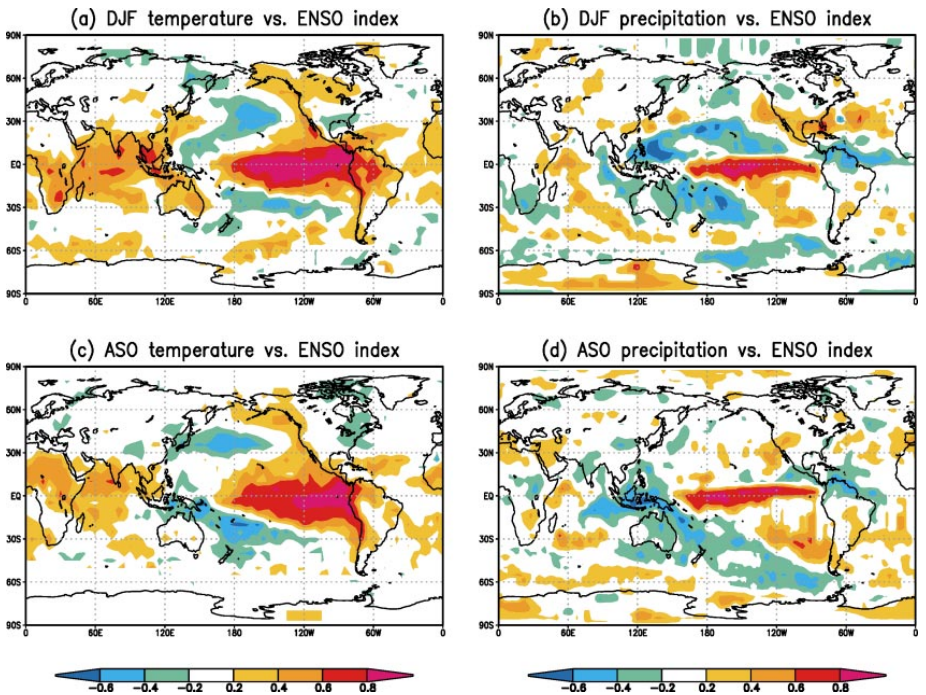


**Figure 3** Correlation coefficients between the ENSO index and (*a*) global temperature in December–February (DJF); (*b*) global precipitation in DJF; (*c*) global temperature in August–October (ASO); (*d*) global precipitation in ASO. Figures are modified from Diaz et al. (32).

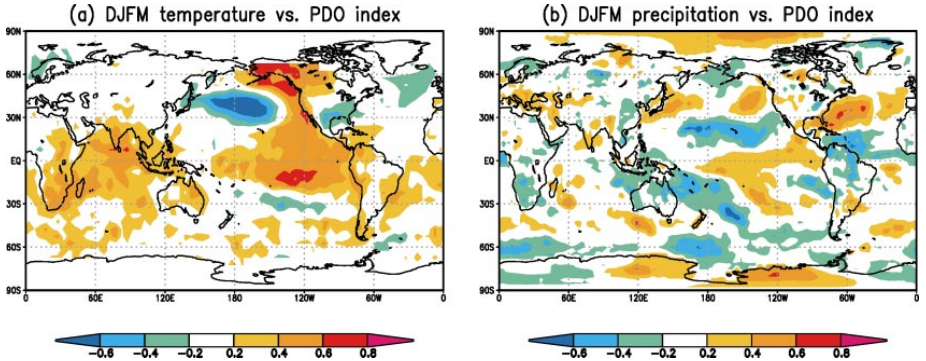


**Figure 4** Same as Figure 2, but for the PDO index. Figure 4*a* uses data from the period 1951–2000, and Figure 4*b* uses data from the period 1979–2001.

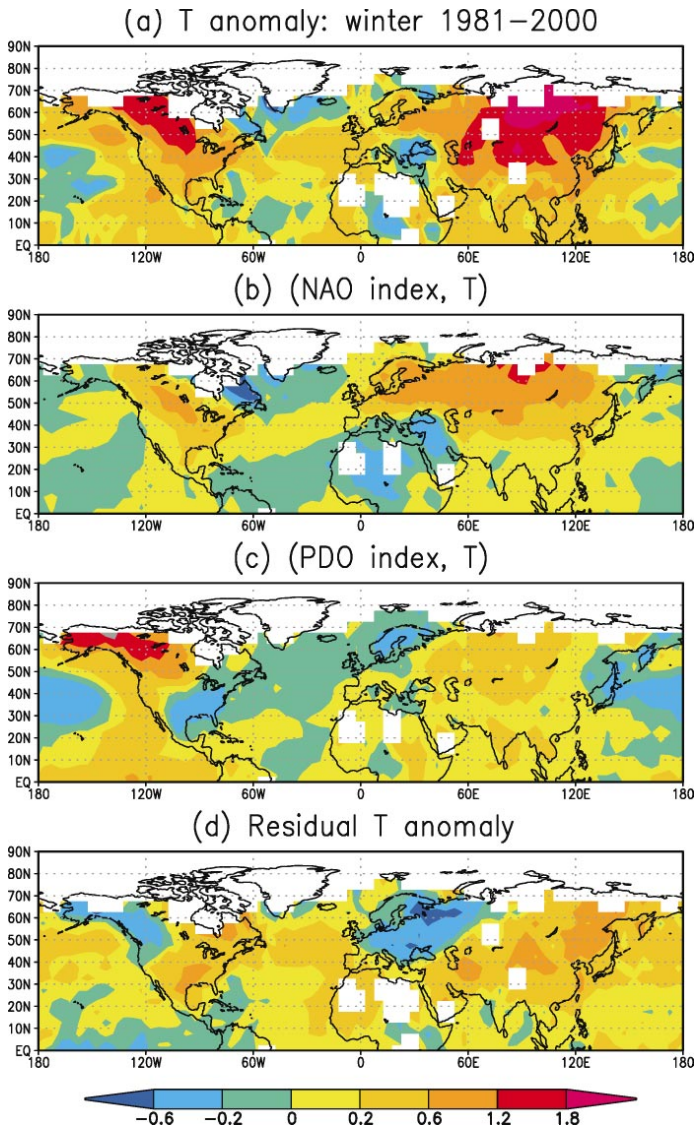


**Figure 6** (*a*) Departure of the winter (December–March) surface temperature averaged during 1981–2000 from the preceding 20-winter average (1961–1980); (*b*) winter temperature anomalies corresponding to a unit increase of the normalized NAO index; (*c*) winter temperature anomalies corresponding to a unit increase of the normalized PDO index; and (*d*) residual temperature anomaly in (*a*) that cannot be explained by the NAO and PDO. The regression analysis in (*b*) and (*c*) are based on data during the period 1951–2000. All temperature units are °C.

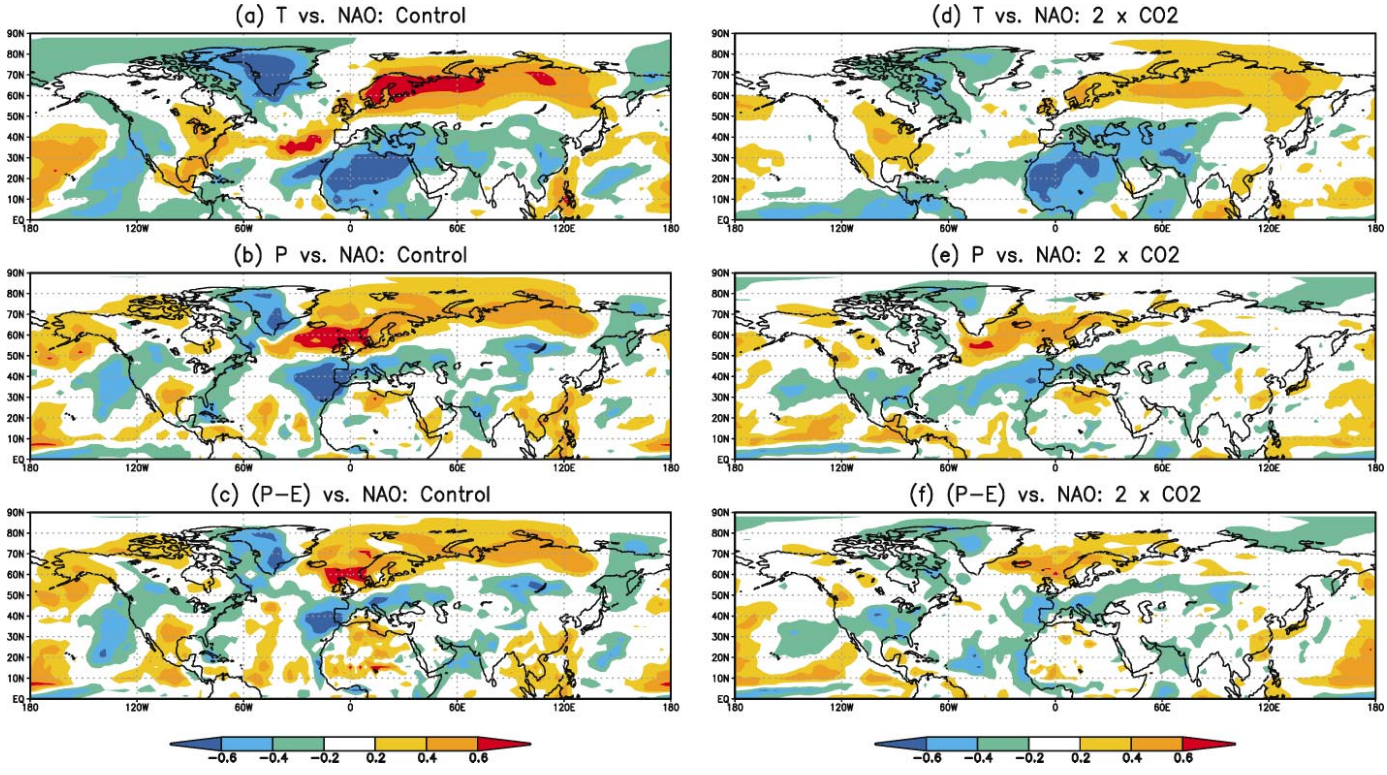


**Figure 8** Correlation coefficients between the NAO index and surface temperature (T), precipitation (P), and fresh water flux (P-E) based on DOE PCM simulations (B04.10 and B04.29). Left panels present results based on a 30-year episode of model integration in the control simulation (B04.10) where $CO_2$ concentration was fixed at 355 ppmv; right panels present results based on the 30-year model integration after the stabilization of $CO_2$ concentration at 710 ppmv in the transient $CO_2$ experiment B04.29. For a sample size of 30, the 5% significance level corresponds to a correlation coefficient of about 0.36.